Applied and Computational Mechanics 8 (2014) 177–186

A comparative study of 1D and 3D hemodynamics in patient-specific hepatic portal vein networks

A. Jonášová[a,*], O. Bublík[a], J. Vimmr[a]

[a] *European Centre of Excellence NTIS — New Technologies for the Information Society, Faculty of Applied Sciences, University of West Bohemia, Univerzitní 8, 306 14 Pilsen, Czech Republic*

Received 16 September 2014; received in revised form 28 November 2014

Abstract

The development of software for use in clinical practice is often associated with many requirements and restrictions set not only by the medical doctors, but also by the hospital's budget. To meet the requirement of reliable software, which is able to provide results within a short time period and with minimal computational demand, a certain measure of modelling simplification is usually inevitable. In case of blood flow simulations carried out in large vascular networks such as the one created by the hepatic portal vein, simplifications are made by necessity.

The most often employed simplification includes the approach in the form of dimensional reduction, when the 3D model of a large vascular network is substituted with its 1D counterpart. In this context, a question naturally arises, how this reduction can affect the simulation accuracy and its outcome. In this paper, we try to answer this question by performing a quantitative comparison of 3D and 1D flow models in two patient-specific hepatic portal vein networks. The numerical simulations are carried out under average flow conditions and with the application of the three-element Windkessel model, which is able to approximate the downstream flow resistance of real hepatic tissue. The obtained results show that, although the 1D model can never truly substitute the 3D model, its easy implementation, time-saving model preparation and almost no demands on computer technology dominate as advantages over obvious but moderate modelling errors arising from the performed dimensional reduction.

Keywords: patient-specific model, blood flow, finite volume method, Windkessel model

1. Introduction

In the last two decades, human medicine has experienced a remarkable boom in the field of computer-aided imaging methods. With all the possibilities offered, for example, by the computed tomography (CT), it is not surprising that the latest efforts of the bioengineering community are directed toward the development of computational software that would help surgeons in their pre-operative planning and/or aid them during difficult and often life-threatening surgeries. However, compared to numerical simulations performed in industry, where a computation may take days or even weeks depending on the complexity of the solved problem, medicine and especially the clinical practice require results within a short time period and with minimal computational demand. With such strict requirements in mind, a development of reliable clinical software is, thus, not easy and it is only natural that a certain measure of simplification is inevitable and, in some cases, even necessary.

The impact of geometry and model simplifications on blood flow simulations is addressed in the present paper, which is one of the results of multidisciplinary research carried out at the University of West Bohemia in close co-operation with the medical doctors of the University

*Corresponding author. Tel.: +420 377 632 397, e-mail: jonasova@ntis.zcu.cz.

Hospital Pilsen and the Faculty of Medicine in Pilsen of the Charles University in Prague. The research, which is directed towards the development of clinical software for liver volumetry [1] and multiscale modelling of tissue perfusion [4], is primarily motivated by the growing need of vascular surgeons to improve the current pre-operative planning of liver surgeries. For example, a surgical removal of a tumour bearing part of the liver (liver resection) is usually performed on the basis of several on-site ultrasound measurements that help to identify the approximate boundaries of functionally independent hepatic segments (e.g., lobes). The final resection line is then chosen as an approximation of these boundaries and perceived as the 'optimal' surgical solution, although in most cases it is anything but. Thus, the need for a more accurate resection approach and with it associated development of a computer-aided pre-operative planning system arose.

Considering the complexity of the solved problem, which involves not only the simulation of vascular blood flow, but also the modelling of hepatic tissue perfusion, see, e.g., [3], several modelling simplifications have to be made. In terms of vascular blood flow, which involves the networks of the portal and hepatic veins (the hepatic arterial flow is neglected), the main simplification takes the form of dimensional reduction. In other words, the hepatic veins are modelled as a network of 1D segments instead of complex 3D structures. The use of this approach in a patient-specific model of human liver is apparent from Fig. 1, which shows the time evolution of contrast medium propagation within portal and hepatic vein systems computed with the help of the aforementioned 1D models of hepatic veins (visualised as black lines in Fig. 1).

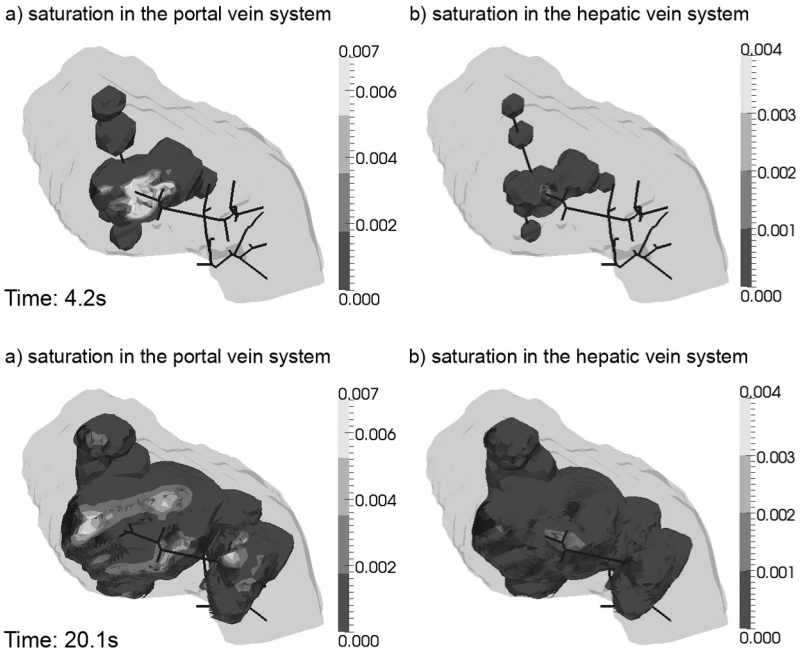

Fig. 1. Example of contrast medium propagation in a patient-specific model of human liver at two selected time instants: $t_1 = 4.2$ s (*top*) and $t_2 = 20.1$ s (*bottom*) (veins shown as black lines) [4]

As the length and distribution of inflow/outflow vessels can significantly affect the resulting tissue perfusion and the subsequent contrast medium propagation, it is crucial to understand the impact of model simplification on the overall simulation accuracy. With this in mind, the main objective of the present study is to compare and assess the flow fields computed by the 3D and 1D models representing two patient-specific hepatic portal vein systems of different complexity.

2. Models and methods

2.1. Hepatic portal vein networks

For the purpose of the present comparative hemodynamical study, we consider two patient-specific portal vein geometries with different levels of complexity and total number of outlets (9 and 39), Fig. 2. To both models, which originate from patient-specific data provided by the courtesy of the University Hospital Pilsen, we shall in the rest of this paper refer to as the simple and complex vascular networks. Their 3D representations shown in Fig. 2 are a result of a semi-automatic reconstruction process carried out on raw image segmentation data prepared by Miroslav Jiřík from the Department of Cybernetics at the University of West Bohemia. The final stage of the reconstruction process involves a smoothing of coarse surface meshes by the well-known Taubin smoothing algorithm [7] and their complete remeshing by the in-house software DICOM2FEM [2]. Finally, tetrahedral computational meshes for the two 3D network models are generated with the help of the software package HyperMesh v11.0 (Altair Engineering, Troy, USA). The number of cells contained in the simple and complex hepatic portal vein networks follows the results of a preliminary mesh sensitivity analysis, which revealed little flow changes in meshes refined near the walls and consisting of at least 816,547 and 2,042,156 cells, respectively. Both these meshes are used in the following blood flow simulations.

For the 1D analogue of the vascular networks mentioned above, the knowledge of lumens and their centres at planes of the CT scans is used, see Fig. 3 (left). To be more specific, each of the two 1D networks consist of simple segments connecting two points situated within the

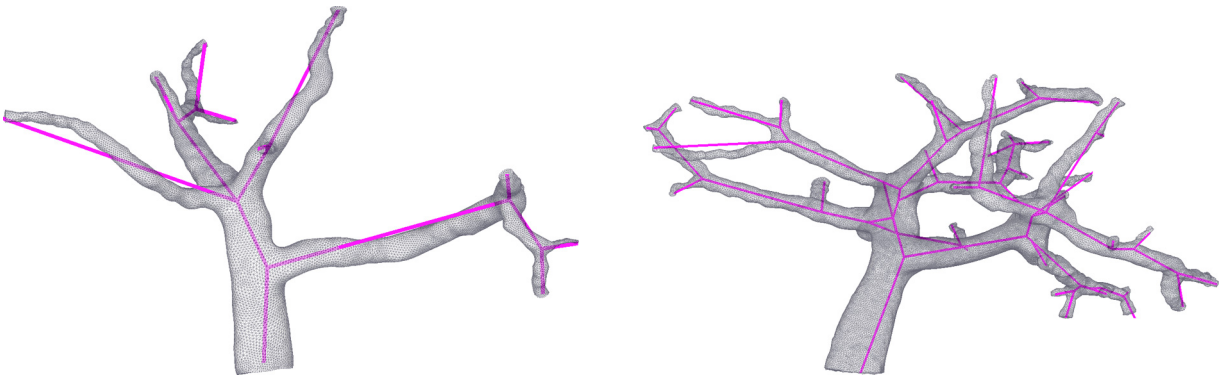

Fig. 2. 1D and 3D reconstructions of simple (*left*) and complex (*right*) hepatic portal vein networks consisting of 9 and 39 outlets, respectively

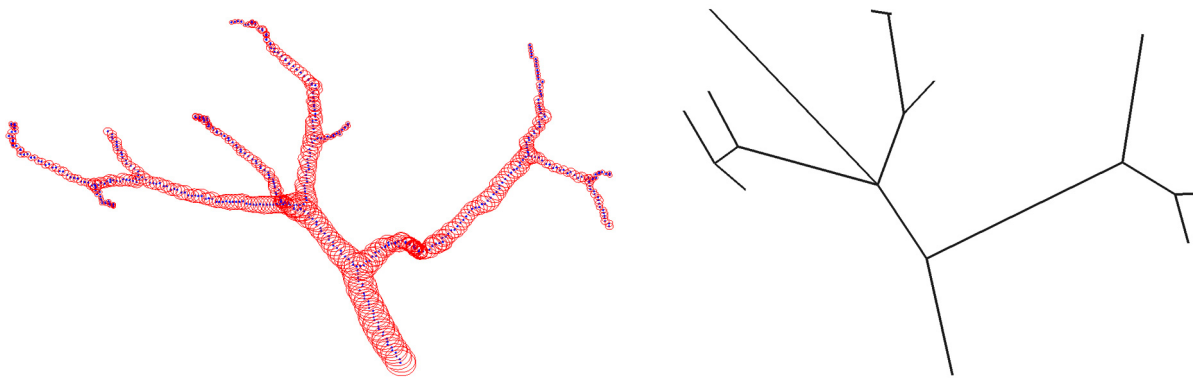

Fig. 3. Reconstruction of the non-segmented simple hepatic portal vein network with lumens and their centres (*left*) and with 1D segments shown as lines (*right*)

vascular network that either represent the inlet, outlet or bifurcation points, Fig. 3 (right). This way, the 1D analogue of the simple and complex hepatic portal vein networks shown in Fig. 2 is created consisting of 18 or 78 segments, respectively. For the purpose of blood flow modelling, which will be addressed later, the segments of the 1D networks also carry the information about their average inner diameter and overall length, both derived from the non-segmented vascular tree model, Fig. 3 (left).

2.2. Three-dimensional blood flow

For the 3D modelling of blood flow in this paper, the assumption of impermeable and inelastic vessel walls is used. The simplification in the form of neglected vascular elasticity is motivated by the fact that blood flow in the hepatic portal vein is known to have a relatively steady character, as illustrated by the examples of velocity waveforms in Fig. 4 measured by an ultrasound Doppler test. As for the impermeability assumption, the objective of the paper is only to consider the upper hierarchy of the perfusion tree, i.e., only the transport of blood into corresponding parts of the liver without the possibility of perfusion is considered. Because of the limitation of the 1D model introduced below, the blood in this study is taken as an incompressible Newtonian fluid with the density of $1\,050\,\mathrm{kg}\cdot\mathrm{m}^{-3}$ and dynamic viscosity of $0.003\,45\,\mathrm{Pa}\cdot\mathrm{s}$.

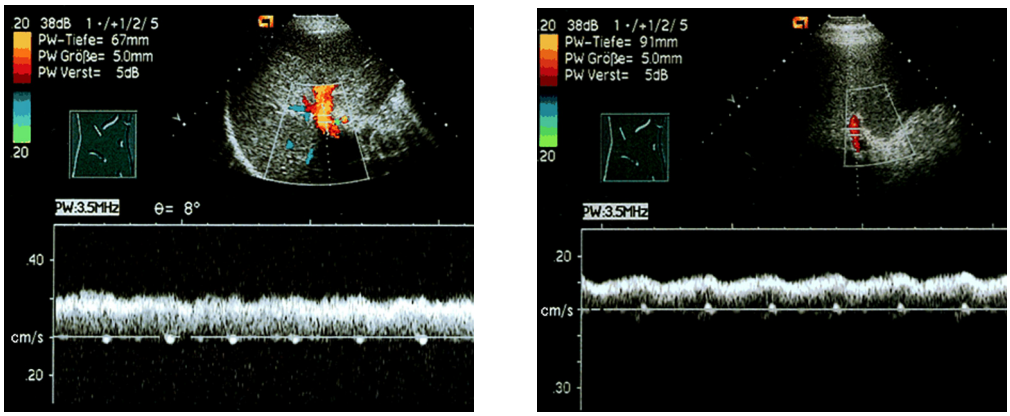

Fig. 4. Examples of Doppler velocity waveforms measured in a human hepatic portal vein

For the description of the blood flow in the reconstructed 3D venous networks, Fig. 2, the complete non-linear system of Navier-Stokes equations for an incompressible Newtonian fluid is used

$$\frac{\partial v_j}{\partial x_j} = 0\,, \tag{1}$$

$$\frac{\partial v_i}{\partial t} + \frac{\partial}{\partial x_j}\left(v_i v_j\right) + \frac{1}{\varrho}\frac{\partial p}{\partial x_i} = \frac{\eta}{\varrho}\frac{\partial^2 v_i}{\partial x_j \partial x_j}\,, \quad i,j = 1,2,3, \tag{2}$$

where t is the time, v_i is the i-th component of the velocity vector $\boldsymbol{v} = [v_1, v_2, v_3]^T$ corresponding to the Cartesian component x_i of the space variables vector $\boldsymbol{x} = [x_1, x_2, x_3]^T$, p is the pressure, ϱ and η are the density and dynamic viscosity of the blood, respectively. The mathematical model given by the system of Eqs. (1)–(2) is numerically solved using our own computational algorithm based on a stabilised variant of the projection method in combination with the cell-centred finite volume method formulated for hybrid unstructured tetrahedral grids. The principle of this algorithm, which we have verified and successfully implemented for the solution of various hemodynamical problems in the past, is described in detail in [8].

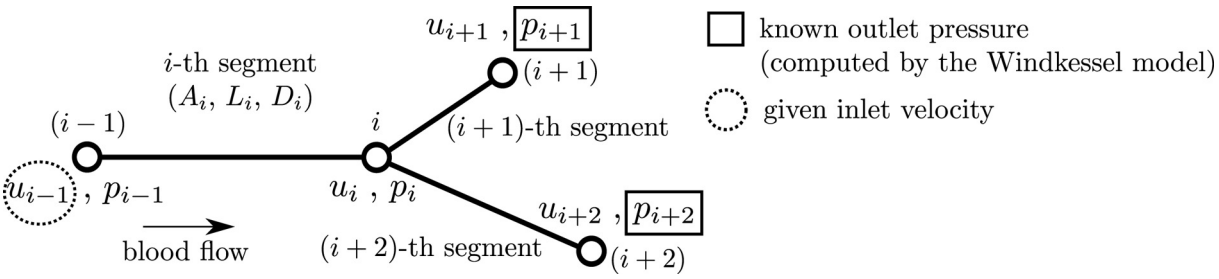

Fig. 5. Schematic drawing of a simple 1D vascular network — a bifurcating vessel

2.3. One-dimensional blood flow

Similarly to 3D flow problem addressed in the previous section, the blood flow in the 1D venous networks is assumed to be a steady flow of a Newtonian incompressible fluid in impermeable and inelastic 1D segments, see Fig. 5. For the modelling of pulsatile 1D blood flow in elastic vessels with variable mechanical properties, we refer the reader, for example, to [6].

Taking the aforementioned modelling simplifications into consideration, the blood flow in the inelastic segments of the 1D venous network is to be governed by the continuity equation and the Bernoulli equation completed with terms representing the friction loss in inelastic tubes. For illustration, let us consider an example of a simple bifurcating vessel, 1D analogue of which is shown in Fig. 5. Here, the motion of blood in the i-th segment of the vessel before the bifurcation can be mathematically described by the following two non-linear algebraic equations

$$A_{i-1}u_{i-1} = A_i u_i \,, \tag{3}$$

$$\frac{1}{2}\varrho u_{i-1}^2 + p_{i-1} = \frac{1}{2}\varrho u_i^2 + p_i + e_i^{\text{loss}} \,, \tag{4}$$

where A_{i-1} is the cross-sectional area of the inlet at the i-th segment, A_i is the average cross-sectional area of the i-th segment, u_i and p_i are the mean velocity and pressure computed at the end of the i-th segment (i.e., at the i-th point). For the approximation of losses originating from the viscous resistance, the term e_i^{loss} in Eq. (4) is computed proportional to the local velocity magnitude, i.e., as $e_i^{\text{loss}} = \frac{1}{2}\varrho u_i^2 \frac{L_i}{D_i}\frac{64}{\text{Re}_i}$, where D_i and L_i are the diameter and length of the i-th segment of the 1D venous network and $\text{Re}_i = u_i D_i \frac{\varrho}{\eta}$ is the corresponding Reynolds number. In the second part of the vessel, Fig. 5, the blood flow after the bifurcation point i is governed by the following three non-linear algebraic equations

$$A_i u_i = A_{i+1}u_{i+1} + A_{i+2}u_{i+2} \,, \tag{5}$$

$$\frac{1}{2}\varrho u_i^2 + p_i = \frac{1}{2}\varrho u_{i+1}^2 + p_{i+1} + e_{i+1}^{\text{loss}} \,, \tag{6}$$

$$\frac{1}{2}\varrho u_i^2 + p_i = \frac{1}{2}\varrho u_{i+2}^2 + p_{i+2} + e_{i+2}^{\text{loss}} \,, \tag{7}$$

where p_{i+1} and p_{i+2} denote known outlet pressures, each computed independently by one three-element Windkessel model, application of which is discussed below in the following section.

By generalising the principles demonstrated above to more complex 1D vascular networks such as the ones considered in this paper, we obtain a system of non-linear algebraic equations that is numerically solved using the well-known Newton method.

2.4. Boundary conditions

To be able to perform a quantitative comparison between the 3D and 1D flow models, we apply the same boundary conditions for both vessel representations. By taking into consideration

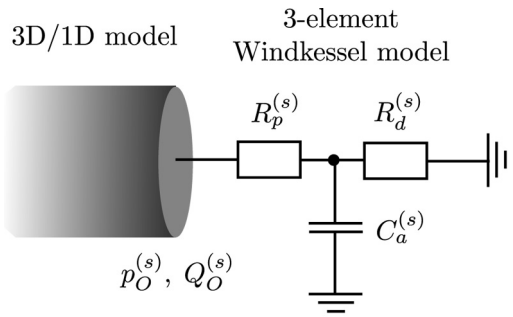

Fig. 6. Schematic drawing of the three-element Windkessel model used as an outflow boundary condition at the s-th outlet of the 3D/1D model of the hepatic portal vein

the relatively steady character of blood flow in real hepatic portal veins (as illustrated by the examples in Fig. 4), an average physiological velocity of $0.325\,\mathrm{m\cdot s^{-1}}$ is prescribed at the inlets of the simple and complex vascular networks considered in this study, Fig. 2. Note that the inlet cross-sectional areas of the 3D/1D models are kept the same, thus, ensuring the prescription of the same inlet flow rate Q_0 in both models.

Because of the difficulties associated with clinical determination of physiological pressure in hepatic portal vein networks, each outlet of the 3D/1D models is coupled with a well-known lumped model — the three-element Windkessel model, schematic drawing of which is shown in Fig. 6. Compared to other modelling approaches such as the prescription of constant outlet pressure, which considering the complex geometry of the venous networks would be difficult to estimate, the Windkessel model is able to approximate the flow resistance of the downstream vascular bed and to provide a physiological value of pressure at all network outlets. For further details on the various types of the Windkessel model and their application, see, e.g., [9].

In general, the mathematical representation of the three-element Windkessel model coupled to the s-th network outlet is given by the following two equations for unknown pressures $p_d^{(s)}$ and $p_O^{(s)}$

$$\frac{\mathrm{d}}{\mathrm{d}t}p_d^{(s)} + \frac{1}{C_a^{(s)}R_d^{(s)}}p_d^{(s)} = \frac{1}{C_a^{(s)}}Q_O^{(s)}\,, \qquad p_O^{(s)} = p_d^{(s)} + R_p^{(s)}\,Q_O^{(s)}\,, \tag{8}$$

where $p_O^{(s)}$ and $Q_O^{(s)}$ are the pressure and flow rate determined at the s-th outlet of the 3D/1D models and $p_d^{(s)}$ is the distal pressure representing the pressure in arterioles and capillaries of the downstream vascular bed (here, the hepatic tissue). Note that the remaining parameters known as the lumped or Windkessel parameters of proximal $R_p^{(s)}$ and distal $R_d^{(s)}$ resistance and capacitance $C_a^{(s)}$ have to be calculated for each outlet prior to the numerical simulation. In this paper, these parameters are taken as a function of the outlet cross-sectional area $A_{\mathrm{out}}^{(s)}$, i.e.,

$$R_p^{(s)} = \frac{k_1}{A_{\mathrm{out}}^{(s)}}, \qquad R_d^{(s)} = \frac{k_2}{A_{\mathrm{out}}^{(s)}}, \qquad C_a^{(s)} = k_3\,A_{\mathrm{out}}^{(s)},$$

where $k_1 = 0.55\times10^4\,\mathrm{Pa\cdot s\cdot m^{-1}}$, $k_2 = 5.54\times10^4\,\mathrm{Pa\cdot s\cdot m^{-1}}$ and $k_3 = 324.6\times10^{-7}\,\mathrm{m\cdot Pa^{-1}}$ are coefficients computed on the basis of data published in [5]. The outlet areas in the 3D and 1D network models are kept the same, thus, ensuring that the response of the relevant Windkessel model will be the same in case of identical outflows.

3. Numerical results

Considering the significance of portal veins in the perfusion tree hierarchy, where their main role is the transport of blood to relevant parts of the liver, the quantitative comparison between the introduced 3D and 1D flow models is aimed at the analysis of outlet flow rates. The flow rate values Q_{3D} and Q_{1D} computed for the simple and complex venous networks are listed in Tables 1 and 2, respectively, with corresponding outlet cross-sectional areas A_{out}. For the position of all the outlets listed in the aforementioned tables, we refer to Figs. 7 and 8, which also contain the information about the blood flow distribution within the two venous networks computed with the help of the three-element Windkessel models. For the sake of better analysis, let us introduce the absolute Δ and relative σ errors defined as

$$\Delta = |Q_{3D} - Q_{1D}|\,, \qquad \sigma = \frac{|Q_{3D} - Q_{1D}|}{Q_{3D}} \cdot 100\,\%\,. \tag{9}$$

Table 1. Overview of all outlet results for the simple portal vein network, as denoted in Fig. 7

outlet No.	A_{out} [mm^2]	flow rate Q [ml · s^{-1}]		Δ [ml · s^{-1}]	σ [%]	σ_A [%]
		3D model	1D model			
1	6.23	4.88	5.51	0.63	12.95	2.07
2	0.74	0.50	0.64	0.13	25.86	0.49
3	6.67	6.47	5.90	0.57	8.85	1.52
4	1.87	1.47	1.64	0.17	11.76	0.57
5	8.36	6.57	7.35	0.79	12.01	2.58
6	4.97	4.73	4.39	0.34	7.11	0.91
7	1.03	0.85	0.89	0.04	4.59	0.12
8	4.88	3.76	4.31	0.55	14.67	1.84
9	4.15	3.28	3.60	0.32	9.77	1.04

Table 2. Overview of selected outlet results for the complex portal vein network, as denoted in Fig. 8

outlet No.	A_{out} [mm^2]	flow rate Q [ml · s^{-1}]		Δ [ml · s^{-1}]	σ [%]	σ_A [%]
		3D model	1D model			
1	1.39	1.38	1.59	0.21	15.32	0.43
4	1.25	1.45	1.28	0.18	12.03	0.30
5	2.49	6.05	5.11	0.94	15.52	0.78
9	1.51	1.96	1.88	0.09	4.54	0.14
10	1.46	1.97	1.73	0.24	12.10	0.36
12	1.30	1.50	1.37	0.12	8.15	0.21
16	1.35	1.48	1.50	0.02	1.39	0.04
19	0.82	0.65	0.54	0.11	17.25	0.28
20	1.03	0.82	0.87	0.05	6.64	0.14
22	1.21	1.38	1.19	0.20	14.39	0.35
23	1.68	2.89	2.30	0.58	20.20	0.68
25	0.74	0.49	0.43	0.06	11.33	0.17
26	1.53	2.00	1.92	0.08	3.90	0.12
30	1.23	1.27	1.25	0.03	2.22	0.06
36	1.92	2.91	3.02	0.10	3.52	0.14
37	1.68	2.00	2.32	0.31	15.63	0.53

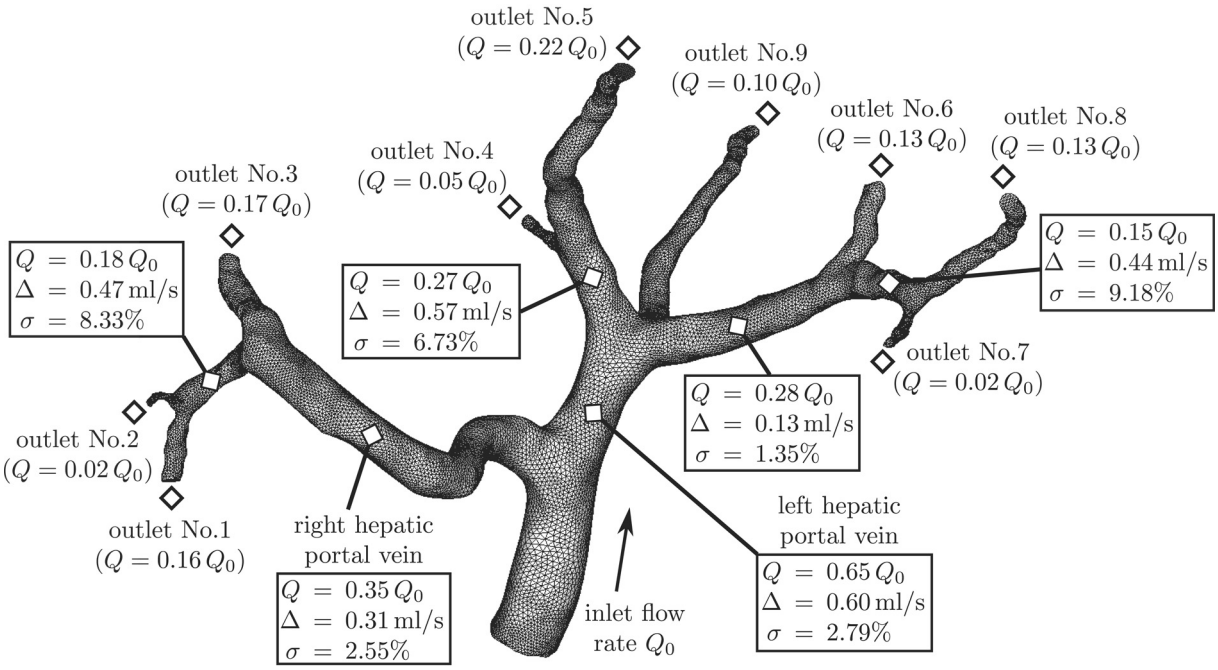

Fig. 7. Blood flow distribution in the simple hepatic portal vein network

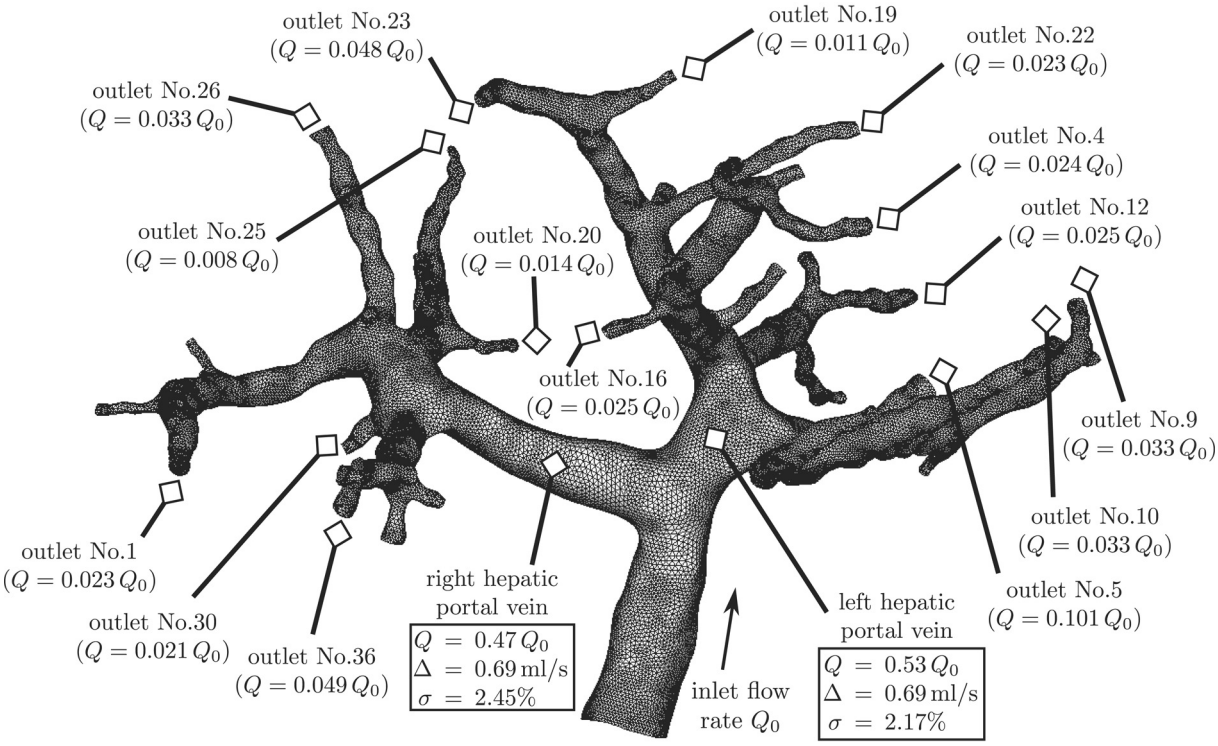

Fig. 8. Blood flow distribution in the complex hepatic portal vein network

On the basis of the errors, it can be observed that, in the case of the simple network (Table 1), the difference between the 3D and 1D flow models is mostly ≤ 0.8 ml/s or, in terms of the relative error, lies between 4 and 26 %. Although the error of about 26 % may seem quite high, it should be noted that it is associated with an outlet of small cross-sectional area, where the accuracy of the 3D flow model is probably not so reliable as at the large-sized outlets.

Therefore, to take into consideration the influence of A_{out} on the computed outflows, let us define the following area-weighted relative error

$$\sigma_A = \frac{A_{\text{out}}}{\sum A_{\text{out}}} \cdot \sigma \,, \tag{10}$$

where A_{out} is the cross-sectional area of the relevant outlet and $\sum A_{\text{out}}$ is the total outlet cross-sectional area of the network (simple model: $\sum A_{\text{out}} = 38.9\,\text{mm}^2$; complex model: $\sum A_{\text{out}} = 49.6\,\text{mm}^2$). Then from Table 1, it can be noted that the outflow at the outlet No. 2 loses its relevance in the overall context and the focus moves to the large-sized outlets No. 1 and 5 — each with the relative error (σ) around 12.5 %.

The same approach as in the simple network is also chosen for the complex one, with the exception that only 16 mostly large-sized outlets are selected for the analysis, Fig. 8. As apparent from the data listed in Table 2, the overall difference between the 3D and 1D flow models in the complex network is restricted to values ≤ 0.3 ml/s, except for the outlets No. 5 and 23, which are characterised by flow differences between 0.5 and 1 ml/s corresponding to $\sigma = 15.5 \div 20.2\,\%$.

4. Conclusions

In this paper, the portal blood flow was simulated in two patient-specific hepatic portal vein networks with the sole purpose to analyse the impact of dimensional reduction on the overall blood flow distribution. Compared to a friction-free 1D flow model, which during a preliminary analysis gave completely unrealistic flow fields with back flow appearing at some outlets, the model presented in this study demonstrated a considerable improvement in our effort to efficiently predict outflow velocities in simple as well as complex vascular networks.

By comparing not only the results obtained for both the 3D and 1D flow models, but also taking into account all the steps preceding any numerical simulation, several advantages $(+)$ and disadvantages $(-)$ of each modelling approach can be noted

- 3D blood flow described by the non-linear system of Navier-Stokes equations (1)–(2):
  - $(-)$ time-consuming model preparation — includes the tasks such as the removal of non-anatomical branches and/or loops, which are usually caused by low-quality CT scans or uneven distribution of the contrast fluid within the blood, and generation of large tetrahedral computational meshes, which depending on the quality of the reconstructed network model, can take several days or even weeks,
  - $(-)$ need for a stable and robust numerical method — requires at least a certain knowledge about special numerical methods used for the solution of the non-linear system of incompressible Navier-Stokes equations,
  - $(-)$ numerical solution of the governing equations is computationally very demanding and strongly depends on the number of tetrahedral elements contained in the computational mesh (with normal computers, the process can take hours or even days to finish),
  - $(+)$ detailed information about the portal hemodynamics at any network location;

- 1D blood flow described by the continuity (3) and Bernoulli equations (4):
  - $(+)$ model preparation consists of only one step — the removal of non-anatomical branches and/or loops,

(+) need for a simple and reliable numerical method — does not require any extra knowledge in the field of computational fluid dynamics (CFD) or programming,
(+) numerical results available within several seconds even with normal (non-high performance) computers,
(−) no detailed information on the flow field is provided outside the network points.

On the basis of the observations made above, a clear conclusion can be drawn. Namely, that despite the existing differences in computed flow fields, which are a natural outcome considering the performed dimensional reduction, the benefits of the 1D approach clearly outweigh its slight inaccuracy when compared to its 3D counterpart. Although the outflow differences (σ mostly between 10 and 20 %) may seem high, it is important to recall the purpose of this study, which is to develop an efficient computational algorithm for the modelling of liver perfusion [3]. Finally, note that because of the efficiency requirement, the 1D flow model does not contain terms that would include 'bifurcation losses'. While these terms can improve the flow estimation (mostly in units of %), it is always at the cost of increased computational time.

Acknowledgements

This study was supported by the project NT13326 of the Ministry of Health of the Czech Republic and by the European Regional Development Fund (ERDF), project "NTIS — New Technologies for the Information Society", European Centre of Excellence, CZ.1.05/1.1.00/02.0090. The help of Miroslav Jiřík from the Department of Cybernetics, University of West Bohemia is also kindly acknowledged.

References

[1] Jiřík, M., Ryba, T., Svobodová, M., Mírka, H., Liška, V., LISA — Liver surgery analyzer software development, Proceedings of the 11th World Congress on Computational Mechanics (WCCM2014), Barcelona, 2014.
[2] Lukeš, V., DICOM2FEM — application for semi-automatic generation of finite element meshes, University of West Bohemia, http://sfepy.org/dicom2fem.
[3] Lukeš, V., Jiřík, M., Jonášová, A., Rohan, E., Bublík, O., Cimrman, R., Numerical simulation of liver perfusion: from CT scans to FE model, Proceedings of the 7th European Conference on Python in Science (EuroSciPy 2014), Cambridge, University of Cambridge, 2014, pp. 79–84.
[4] Jonášová, A., Rohan, E., Lukeš, V., Bublík, O., Complex hierarchical modeling of the dynamic perfusion test: Application to liver, Proceedings of the 11th World Congress on Computational Mechanics (WCCM2014), Barcelona, 2014, pp. 3 438–3 449.
[5] Sankaran, S., Moghadam, M. E., Kahn, A. M., Tseng, E. E., Guccione, J. M., Marsden, A. L., Patient-specific multiscale modeling of blood flow for coronary artery bypass graft surgery, Annals of Biomedical Engineering 40 (2012) 2 228–2 242.
[6] Sherwin, S. J., Franke, V., Peiró, J., Parker, K., One-dimensional modelling of a vascular network in space-time variables, Journal for Engineering Mathematics 47 (3–4) (2003) 217–250.
[7] Taubin, G., A signal processing approach to fair surface design, Proceedings of the 22nd annual conference on Computer graphics and interactive techniques — ACM SIGGRAPH 95, New York, 1995, pp. 351–358.
[8] Vimmr, J., Jonášová, A., Bublík, O., Numerical analysis of non-Newtonian blood flow and wall shear stress in realistic single, double and triple aorto-coronary bypasses, International Journal for Numerical Methods in Biomedical Engineering 29 (10) (2013) 1 057–1 081.
[9] Westerhof, N., Lankhaar, J.-W., Westerhof, B. E., The arterial Windkessel, Medical & Biological Engineering & Computing 34 (8) (2009) 1 049–1 064.